ANTICANCER RESEARCH *40*: 4907-4912 (2020)
doi:10.21873/anticanres.14493

Luteolin Induces Cytotoxicity in Mix Cellularity Classical Hodgkin's Lymphoma *via* Caspase Activated-cell Death

RAJENDRA GHARBARAN[1,2], ENYUAN SHANG[1], ONYEKWERE ONWUMERE[2,3], NAOMI CODRINGTON[2], EVANGELINA DANKWA SARPONG[1,2] and STEPHEN REDENTI[2,3]

[1]*Department of Biological Sciences, Bronx Community College/The City University of New York, Bronx, NY, U.S.A.;*
[2]*Department of Biological Sciences, Lehman College/City University of New York, Bronx, NY, U.S.A.;*
[3]*Biology Doctoral Program, The Graduate School and University Center, City University of New York, New York, NY, U.S.A.*

Abstract. *Background/Aim: We investigated the effects of luteolin (LUT) on classical Hodgkin's lymphoma (cHL), since such studies in malignant lymphomas are lacking. Materials and Methods: Effect of LUT on cell growth was assessed with water-soluble tetrazolium 1 (WST-1) cell proliferation assay and automated hemocytometry on trypan blue-exclusion assay. Cell death was investigated with acridine orange/ethidium bromide live-dead assay, propidium iodide (PI) flow cytometry, and Annexin-V-PI microscopy. Caspase activation was studied using CellEvent Caspase-3/7 Green detection reagent. High resolution immunofluorescence microscopy was used to detect cleaved-PARP-1. Results: LUT induced a dose-dependent decrease in the growth of KMH2 and L428 cells, cellular models of mix-cellularity (MC) and nodular sclerosis (NS) cHL, respectively. However, LUT induced cell death only in KMH2, at a higher concentration, and this was associated with caspase activation and cleaved PARP-1. Conclusion: LUT induces cytotoxicity in the MC-cHL cellular model KMH2 via caspase activation.*

While current frontline treatment regimens, which include ABVD (adriamycin, bleomycin, vinblastine, and dacarbazine) result in a high cure rate in classical Hodgkin's lymphoma (cHL) (1), disease relapse, refractory disease, treatment-related toxicities, and development of secondary neoplasms, remain significant concerns (2). In addition, only less than 50% patients who fail frontline therapy and subsequently treated with either autologous stem cell transplant (ASCT) or Brentuximab vedotin show clinical responses (3, 4). To mitigate these concerns associated with poor clinical responses in cHL, one line of research is focused on the development and discovery of new therapeutic approaches.

Luteolin (3,4,5,7-tetrahydroxy flavone, LUT), a flavonoid found in common foods, has been widely studied for its anti-cancer potential, as demonstrated in studies in multiple human malignancies such as lung, breast, glioblastoma, prostate, colon, and pancreatic cancers (5). LUT has been shown to trigger apoptosis (6, 7), inhibit cell growth, stimulate cell cycle arrest (6, 7) and disrupt metastasis (8) and cell migration (8, 9). However, although increased dietary intake of flavonoids was associated with reduced risk of disease occurrence in non-Hodgkin's lymphoma, (10), there is very limited information about the effects of LUT on hematological malignancies. In myeloid leukemia, LUT-induced apoptosis is modulated by the differential expression of the oncoprotein PTTG1 (pituitary tumor-transforming gene 1) (11). In multiple myeloma, LUT causes cell death by apoptosis and autophagy (12). To date however, there is no study on the effect of LUT on malignant lymphomas. Therefore, the goal of this current study was to investigate the potential anti-cancer effects of LUT on cHL.

Materials and Methods

Drug. LUT was purchased from SelleckChem (Houston, TX, USA) and dissolved in DMSO (Sigma-Aldrich, St. Louis, MO, USA) to prepare a 50-mM stock, which was aliquoted and stored at −20˚C until ready to be used. All working stocks of LUT were prepared to a final concentration of 0.01% DMSO.

Cell lines and cell cultures. The human HRS-derived cell lines KMH2 and L428 were obtained from the German Collection of Microorganisms and Cell Cultures (DSMZ), Department of Human and Animal Cell Cultures, Braunschweig, Germany. L428 and KMH2 were cultured in RPMI 1640 medium supplemented with

Correspondence to: Rajendra Gharbaran, Ph.D., Department of Biological Sciences, Bronx Community College of The City University of New York, Bronx, NY 10453, U.S.A. Tel: +1 7182893026, e-mail: rajendra.gharbaran@bcc.cuny.edu

Key Words: Luteolin, Hodgkin's lymphoma, cancer, mix cellularity classical Hodgkin's lymphoma.

10% heat-inactivated fetal bovine serum (FBS) (Gibco, Gaithersburg, MD, USA), 1% L-glutamine (Thermo Fisher Scientific, Waltham, MA, USA) and penicillin/streptomycin (Thermo Fisher Scientific). Cells used in these experiments were from an early passage (L428 and KMH2 passage 3), and tested negative for mycoplasma infection (13, 14). All cells were maintained in a humid environment of 5% CO_2 at 37˚C.

WST-1 cell proliferation assay. Cell growth was assessed with WST-1 cell proliferation assay (Roche; Branchburg, NJ, USA), according to manufacturer's instructions and as described by Gharbaran *et al*. (15). One hundred μl of 1×10^5 cells/ml were seeded in a 96-well plate, and incubated overnight. Cells were then treated with 0, 20, 40, and 80 μM of LUT or DMSO for 48 h. The treated cells were incubated with 10 μl WST-1 reagent for 3 h following standard cell culture conditions. Absorbance was read at 450 nm on a Synergy H1 Hybrid microplate reader (BioTek Instruments; Winooski, VT, USA). Cell growth (in percentages, %) was computed as a ratio of the absorbance (A450) of LUT-treated cells to the absorbance of the DMSO control. The assay principle is based on the conversion of the tetrazolium salt WST-1 into a colored dye by mitochondrial dehydrogenase enzymes.

Trypan blue exclusion assay and hemocytometry. LUT-induced changes in cell viability and cell growth were determined by trypan blue exclusion assay and hemocytometry using an EVE automated cell counter (NanoEnTek; Guro-gu, Seoul, Korea), according to the manufacturer's instructions. One hundred μl of 1×10^5 cells/ml seeded in 96-well plates were treated with 0, 20, 40 and 80 μM LUT or DMSO, for 48 h. Ten μl of a suspension of treated cells were mixed with 10 μl 0.4% trypan blue. Ten μl of this mixture were then loaded into a counting chamber.

Acridine orange and ethidium bromide live/dead assay. Acridine orange (AO)-ethidium bromide (EtBr)—AO/EtBr-- assay was used to determine cell death. One hundred μl of 1×10^5 cells/ml were seeded in 96-well plates overnight and then treated with 40 μM LUT or vehicle, for 48 h. Four μl of a solution consisting of 10 μg/ml each of AO and EtBr were added to each well of treated cells and immediately imaged. In this assay, the membrane-permeable AO stained live cells green and EtBr, which is membrane-impermeable, stained the nuclei of dead cells orange to red.

Annexin V FITC- propidium iodide assay. Annexin V-propidium iodide staining was carried out using Annexin V FITC Assay Kit (Cayman Chemicals; Ann Arbor, MI, USA), according to the manufacturer's instructions. One hundred μl of 1×10^5 cells/ml were seeded in 96-well plates overnight and treated with 40 μM LUT or vehicle, for 48 h. Treated cells were transferred to a microfuge tube and collected by centrifugation at 400 × *g* for five min at room temperature, and then resuspended in 100 μl 1 X binding buffer. Cells were then centrifuged as described and incubated in 50 μl Annexin V FITC/Propidium Iodide Staining Solution for 10 min at room temperature in a dark chamber. Stained cells were collected by centrifugation and resuspended in binding buffer. Cells were then transferred to chamber slides containing poly D-lysine for microscopy analysis.

Flow cytometry analysis and detection of sub-G1 cell population. Cells were seeded into 6-well plates at 1×10^5 cells/well, incubated overnight, and then treated with 40 μM LUT for 48 h. Harvested cells were fixed in 70% ethanol, collected by centrifugation, and re-suspended in PBS containing 10 μg/ml Propidium Iodide (PI) and 300 μg/ml RNAse A (Cell Signaling; Danvers, MA, USA) for 15 min at room temperature. The stained cells were analyzed on a BD LSRII flow cytometer and collected data were analyzed by FlowJo software (version 10; Tree Star, Ashland, OR, USA). In this assay, fragmented DNA was not retained following ethanol fixation and such cells were detected as the sub-G_1 population (apoptotic cells).

Detection of caspase activities. Caspase3/7 activities were analyzed using the CellEvent Caspase-3/7 Green Detection Reagent (Life Technologies, CA, USA), according to manufacturer's instructions. Cells seeded into 96-well plates at a density of 1×10^5 cells/ml were incubated overnight, and then treated with 40 μM LUT or DMSO for 48 h. Cells were then incubated with CellEvent Caspase-3/7 Green Detection Reagent to a final concentration of 2 μM for 30 min, following standard cell culture conditions. These experiments included LUT-treated cells pre-incubated for 1 h with the pan-caspase inhibitor Z-VAD-FMK (BioVision; Milpitas, CA, USA).

Microscopy. Microscopy was carried out as previously described (15). Images for live/dead assay, casp3/7 activation, and annexin V-FITC/PI analyses, were generated from randomly selected fields. About 5 to 10 fields were imaged per dose. Cell counts on images were carried out manually, blindly, by independent counters (counts were carried out by researchers who did not know what sample the images represent).

Cellular immunofluorescence. Immunofluorescence was carried out according to Gharbaran *et al*. (15) with some modifications. Cells adhered to poly-D lysine (Sigma-Aldrich) coated number 1 coverslips for 30 min in a humid chamber at 37˚C in 5% CO_2, rinsed 1 × with PBS, and then fixed for 20 min with 3.7% paraformaldehyde (Electron Microscopy Sciences 15710, Hatfield, PA, USA). Fixed cells were permeabilized with 0.1% PBS-Triton X-100 (Sigma–Aldrich) for 30 min, then blocked for 30 min in 1% normal goat serum followed by incubation with anti-cleaved PARP-1 rabbit monoclonal antibody (clone Y34, Abcam; Cambridge, MA, USA) diluted 1:200 in blocking buffer for 1 h, followed by three rinses for 5 min each with 0.1% PBS-Tween 20. The cells were next incubated with Dylight-488 labeled secondary antibody (Jackson ImunoResearch; West Grove, PA, USA) diluted at 1:500 in blocking buffer, from a stock prepared in 50% glycerol. Stained cells were mounted in ProLong Gold anti-fade reagent containing DAPI (Life Technologies, Carlsbad CA, USA) and images were captured with a CoolSNAP HQ2 CCD camera (Cool SNAP EZ, Photometrics, Tucson, AZ, USA) coupled to a Nikon Ti Eclipse inverted microscope (Melville, NY, USA).

Statistical analyses. Data analyses were performed using SAS 9.1.3 (Cary, NC, USA) and StatView 5 (Cary, NC, USA). Analysis of variance (ANOVA) and F statistics were used to determine significant differences between the means as defined by $p<0.05$. Data obtained from the assays on cell growth, cell viability, AO/EtBr, Annexin V-PI, caspase3/7, and flow cytometry, are presented as plus or minus standard error of the mean (±SEM). For the cell growth assay, the mean per dose was determined from triplicates. Each experiment was repeated at least three times.

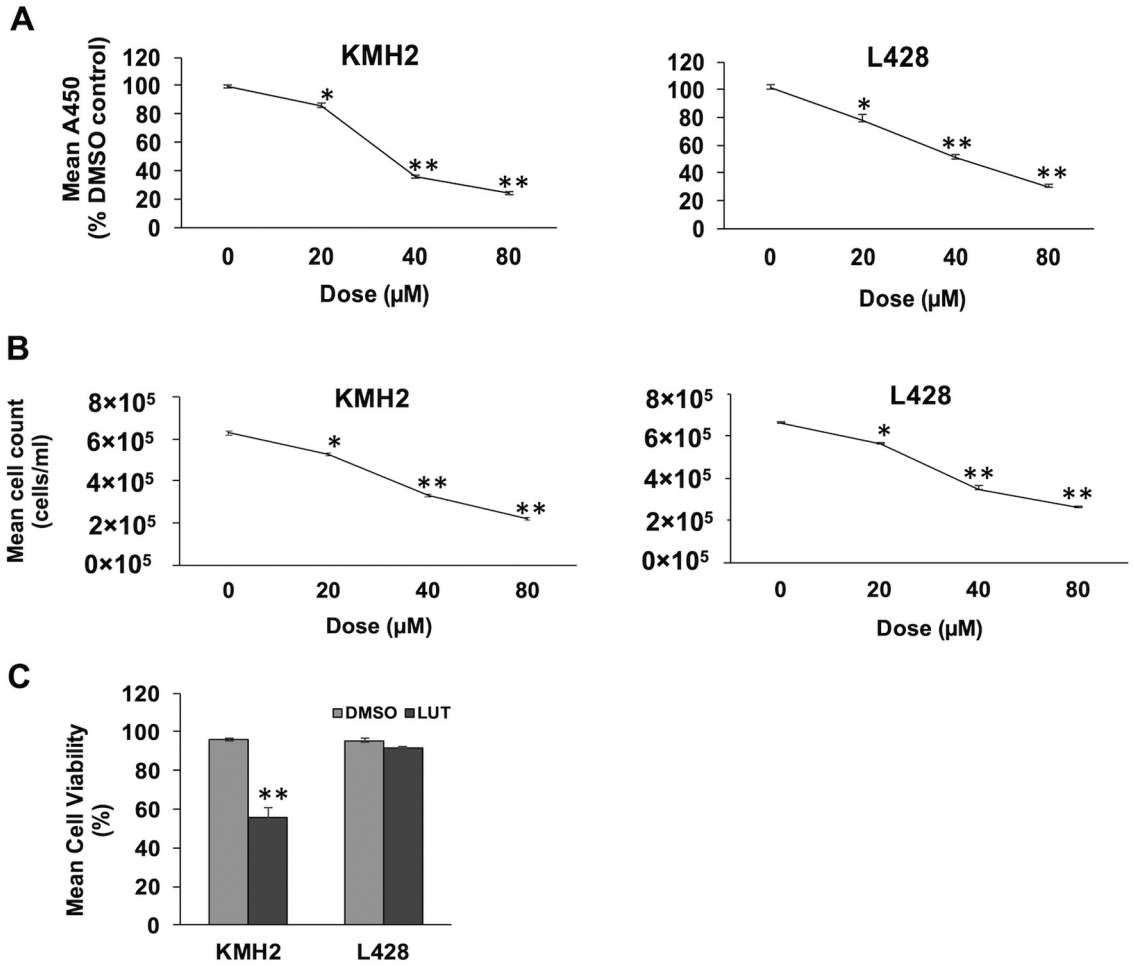

Figure 1. *Effect of luteolin (LUT) on the growth of KMH2 and L428 cells. A. WST-1 analyses of LUT induced dose-dependent decrease in the growth of KMH2 and L428 cells. B. Automated hemocytometry data on LUT-induced dose-dependent decrease in cell growth. C. Automated hemocytometry on trypan blue-stained cells revealed a significantly lower proportion of viable KMH2 cells compared to L428, after treatment with 40 μM of LUT. Cells were treated with 0, 20, 40, and 80 μM of LUT for 48 h. Cell growth was evaluated independently with WST-1 cell proliferation assay and trypan blue exclusion assay. Significantly different at *p<0.05 and **p<0.01 as compared to the control group. Results are presented as the mean±standard error.*

Results

Effect of LUT on cell growth. WST-1 cell proliferation assay and automated hemocytometry on trypan blue exclusion assay were used to independently evaluate the effects of LUT on cell growth, following treatment for 48 h. LUT significantly inhibited the growth of both KMH2 ($p<0.00001$) and L428 ($p<0.00001$) cells in a dose-dependent manner (Figure 1A). Automated hemocytometry after trypan blue exclusion assay revealed a similar trend (Figure 1B). However, although both cell lines showed comparable changes in cell growth at higher doses of LUT, the automated hemocytometry detected a lower proportion of KMH2 viable cells (52%) compared to L428 (92%) (Figure 1C). Microscopic examination of treated cells with higher doses of LUT revealed a larger proportion of KMH2 cells with compromised membranes compared to L428 cells (data not shown). These results indicated that LUT, at higher doses, may be strongly inducing death of KMH2 cells, a cellular model of MC-cHL.

LUT induces apoptosis in KMH2. LUT-treated KMH2 cells were next studied for cell death. AO/EtBr live-dead staining of KMH2 cells treated with 40 μM LUT for 48 h showed increased cell death. As shown in Figure 2A, the mean percent of EtBr-positive cells (stained red) was 33.6% (±2.08%) compared to DMSO control (7.27%±1.09%) ($p<0.00001$). LUT-induced cell death was further investigated with Annexin V-PI microscopy. As shown in Figure 2B, Annexin V-PI positive cells were significantly higher in LUT-treated KMH2

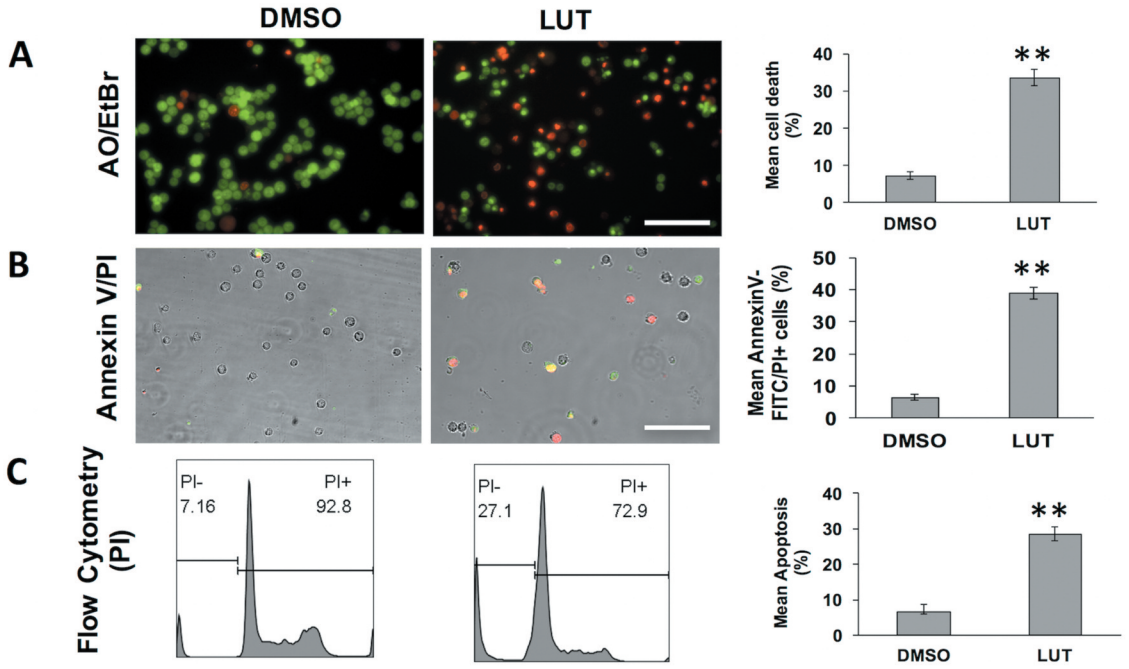

Figure 2. *Effect of LUT on death of KMH2 cells. A. Acridine orange/ethidium bromide (AO/EtBr) staining detected significantly higher number of dead cells (red) due to LUT treatment compare to DMSO. B. Significantly higher proportion of Annexin V/PI-positive cells were detected after LUT treatment compared to DMSO. C. Flow cytometry-PI detected higher levels of apoptosis after LUT treatment compared to DMSO. Cells were treated with 40 μM of LUT or DMSO for 48 h. Significantly different at *p<0.05 and **p<0.01 as compared to the control group. Results are presented as the mean±standard error.*

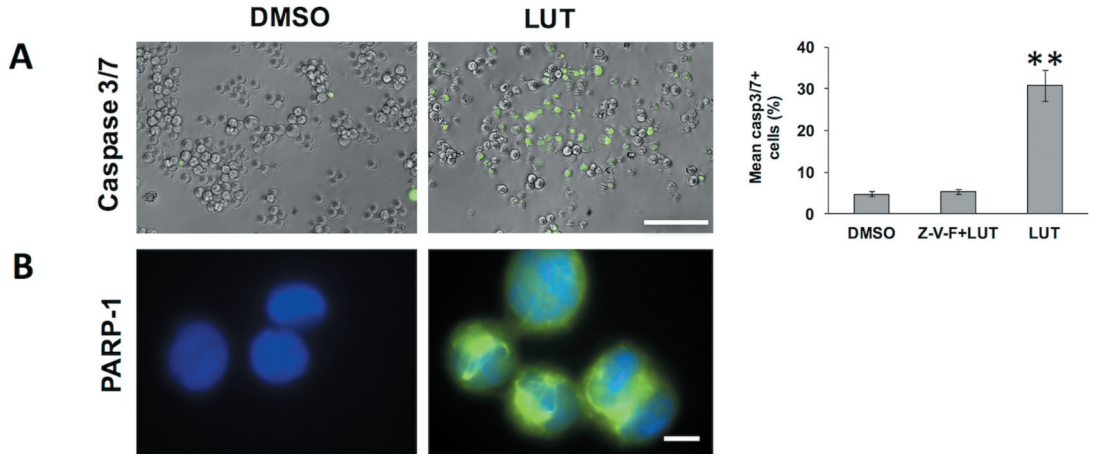

Figure 3. *Effect of LUT on caspase and PARP-1 activities in KMH2 cells. A. LUT treatment resulted in a significantly higher number of caspase3/7-positive cells. B. Cleaved PARP-1 (green fluorescent) was detected in LUT-treated cells, but was absent in DMSO-treated control cells. Cells were treated with 40 μM of LUT or DMSO for 48 h and analyzed using CellEvent Caspase-3/7 Green Detection Reagent and anti-cleaved PARP-1 immunofluorescence microscopy. Significantly different at **p<0.01 compared to the control group. Results are presented as the mean±standard error. Scale bar in A is 100 μm, and that for B is 10 μm.*

(38.9%±1.92) compared to DMSO-treated cells (6.55%±0.94%) (p<0.00001). Additionally, flow cytometry analysis of ethanol-fixed PI-stained cells showed a statistically significantly higher percentage of LUT-treated KMH2 cells in the sub-G_1 phase (28.6%±2.00%) compared to DMSO-treated cells (7.16%±0.43) (p<0.00001) (Figure 2C).

Activation of caspase activities in KMH2 and detection of cleaved PARP-1. To gain insights into the putative mechanism of LUT-induced cell death, LUT-treated KMH2 cells were assessed for caspase activities. A caspase3/7-specific fluorochrome detection dye revealed significantly higher levels of caspase3/7-postive cells (stained green) in the LUT-treated KMH2 cells (30.7%±3.7%) compared to either DMSO (4.77%±0.63%) or LUT-treated cells pre-incubated with the pan-caspase inhibitor Z-VAD-FMK (5.34%±0.58%) ($p<0.00001$) (Figure 3A). Since KMH2 cells are caspase 3-deficient (16), it is likely that LUT triggered activation of caspase7 in this cell line.

PARP-1, a DNA-repair enzyme, is a cellular substrate for caspases (17) and both PARP-1 cleavage and caspase7 activation have been observed in KMH2 cells treated with doxorubicin and camptothecin (18). LUT-treated KMH2 cells were therefore studied for PARP-1 activation. High-resolution immunofluorescent imaging of LUT-treated KMH2 cells, using an anti-cleaved PARP-1 monoclonal antibody, showed a strong nuclear focal staining pattern of cleaved PARP-1 expression, which was absent in the DMSO-treated control cells (Figure 3B). Visible green fluorescent puncta in Figure 3B may reflect regions where cleaved PARP-1 interacted with damaged DNA. These results suggest that LUT-induced cell death in KMH2 proceeded through caspase-activated apoptosis.

Discussion

LUT, a flavonoid found in common foods, has been widely studied for its anti-cancer potential. LUT has been implicated in the induction of apoptosis (6, 7), inhibition of cell growth and cell cycle arrest (6, 7), and disruption of metastasis (8) and cell migration (8, 9). Among hematological malignancies, there is only a paucity of information on the anti-cancer activities of LUT. In myeloid leukemia, LUT-induced leukemic apoptosis is modulated by the differential expression of the oncoprotein PTTG1 (pituitary tumor-transforming gene 1) (11). In multiple myeloma, LUT treatment resulted in cell death by apoptosis and autophagy (12). Presently, there is little or no information on the effect of LUT on lymphoma.

The current study showed that LUT suppresses the growth of cHL, *in vitro*. Both cell lines, KMH2 and L428, showed dose-dependent cell growth responses to LUT treatment (Figure 1A and B). However, automated hemocytometry on trypan blue-stained LUT-treated cells revealed a significantly lower proportion of viable KMH2 cells compared with L428, at higher doses (Figure 1C). Microscopic examination of LUT-treated KMH2 cells revealed cells with compromised membranes. Cell death analysis using AO/EtBr staining, Annexin V-PI microscopy, and flow cytometry-PI supported the LUT-induced apoptosis of KMH2 cells at higher doses (Figure 2). A caspase3/7-specific fluorescent stain detected significantly higher levels of caspase-positive LUT-treated KMH2, at 40 μM (Figure 3A). Because KMH2 is caspase3-deficient (16), it is likely that LUT causes activation of caspase7 in this cell line. Upon induction of caspase activation-associated apoptosis, leading to extensive and irreparable DNA damage, PARP-1 is rapidly cleaved by effector caspases (19, 20), presumably to limit further DNA damage. It is presumed that the resulting C-terminal fragment is shuttled out of the nucleus, leaving the N-terminal fragment nuclear-bound. In addition, a previous study showed that treatment of KMH2 cells with escalating concentrations of camptothecin and doxorubicin triggered increased PARP-1 cleavage, as shown by western blot analysis using a polyclonal antibody that detected both the cleaved and the un-cleaved protein (18). Our result showed, using a specific monoclonal antibody in high-resolution immunofluorescence microscopy, nuclear focal staining of cleaved-PARP-1 (Figure 3B). These observations suggest that LUT in part, suppresses viability of KMH2 *via* caspase activation.

Our results also showed disparate responses of either cell line, KMH2 or L428 to LUT. Both cell lines showed similar growth-restricting responses to LUT (Figure 1A and B), but KMH2 cells displayed lower viability compared to L428 at higher doses of the compound (Figure 1C). Subsequent analyses revealed the induction of apoptosis in KMH2 cells, which was not evident in L428 cells. Similar disparate responses of these two cell lines to the same compound have been observed in other studies. Celastrol inhibits proliferation, induces apoptosis and growth arrest of KMH2 *via* caspase3/7 activation, whereas L428 cells were recalcitrant to this compound (21). The difference in cellular responses of either KMH2 or L428 to the same drug may be related to different subtypes of cHL. KMH2 is a cellular model of MC-cHL, and L428 of nodular sclerosis cHL. However, it is not clear if these cHL subtypes exhibit differential responses to chemotherapeutic drugs, *in vivo*.

Conflicts of Interest

The Authors declare no conflicts of interest regarding this study.

Authors' Contributions

RG conceptualized project, designed and conducted experiments, interpreted data and wrote manuscript. ES, OO, NC, and EDS conducted experiments. RG, ES, OO, SR interpreted data. All Authors read and approved the final manuscript.

Acknowledgements

Support for this project was provided in part by a PSC-CUNY Award, jointly funded by The Professional Staff Congress and The City University of New York (Award #: TRADB-48-360), and The City University of New York Community College Research Grant (Award #: 80212-03-17).

References

1 Meyer RM, Gospodarowicz MK, Connors JM, Pearcey RG, Wells WA, Winter JN, Horning SJ, Dar AR, Shustik C, Stewart DA, Crump M, Djurfeldt MS, Chen BE, Shepherd LE, Group NCT and Eastern Cooperative Oncology G: Abvd alone versus radiation-based therapy in limited-stage hodgkin's lymphoma. N Engl J Med 366(5): 399-408, 2012. PMID: 22149921. DOI: 10.1056/NEJMoa1111961

2 Pavlovsky S: Treatment options in early stages of hodgkin's lymphoma, high cure rate with lower short and long-term toxicity. Hematology *10(Suppl 1):* 3-5, 2005. PMID: 16188621. DOI: 10.1080/10245330512331389700

3 Majhail NS, Ness KK, Burns LJ, Sun CL, Carter A, Francisco L, Forman SJ, Bhatia S and Baker KS: Late effects in survivors of hodgkin and non-hodgkin lymphoma treated with autologous hematopoietic cell transplantation: A report from the bone marrow transplant survivor study. Biol Blood Marrow Transplant *13(10)*: 1153-1159, 2007. PMID: 17889351. DOI: 10.1016/j.bbmt.2007.06.003

4 Chen R, Gopal AK, Smith SE, Ansell SM, Rosenblatt JD, Savage KJ, Connors JM, Engert A, Larsen EK, Huebner D, Fong A and Younes A: Five-year survival and durability results of brentuximab vedotin in patients with relapsed or refractory hodgkin lymphoma. Blood *128(12)*: 1562-1566, 2016. PMID: 27432875. DOI: 10.1182/blood-2016-02-699850

5 Imran M, Rauf A, Abu-Izneid T, Nadeem M, Shariati MA, Khan IA, Imran A, Orhan IE, Rizwan M, Atif M, Gondal TA and Mubarak MS: Luteolin, a flavonoid, as an anticancer agent: A review. Biomed Pharmacother *112:* 108612, 2019. PMID: 30798142. DOI: 10.1016/j.biopha.2019.108612

6 Park SH, Ham S, Kwon TH, Kim MS, Lee DH, Kang JW, Oh SR and Yoon DY: Luteolin induces cell cycle arrest and apoptosis through extrinsic and intrinsic signaling pathways in mcf-7 breast cancer cells. J Environ Pathol Toxicol Oncol *33(3)*: 219-231, 2014. PMID: 25272060. DOI: 10.1615/jenvironpatholtoxicoloncol.2014010923

7 Wang F, Gao F, Pan S, Zhao S and Xue Y: Luteolin induces apoptosis, g0/g1 cell cycle growth arrest and mitochondrial membrane potential loss in neuroblastoma brain tumor cells. Drug Res (Stuttg) *65(2)*: 91-95, 2015. PMID: 24831243. DOI: 10.1055/s-0034-1372648

8 Cook MT, Liang Y, Besch-Williford C and Hyder SM: Luteolin inhibits lung metastasis, cell migration, and viability of triple-negative breast cancer cells. Breast Cancer (Dove Med Press) *9:* 9-19, 2017. PMID: 28096694. DOI: 10.2147/BCTT.S124860

9 Zhao Y, Yang G, Ren D, Zhang X, Yin Q and Sun X: Luteolin suppresses growth and migration of human lung cancer cells. Mol Biol Rep *38(2)*: 1115-1119, 2011. PMID: 20589534. DOI: 10.1007/s11033-010-0208-x

10 Frankenfeld CL, Cerhan JR, Cozen W, Davis S, Schenk M, Morton LM, Hartge P and Ward MH: Dietary flavonoid intake and non-hodgkin lymphoma risk. Am J Clin Nutr *87(5)*: 1439-1445, 2008. PMID: 18469269. DOI: 10.1093/ajcn/87.5.1439

11 Chen PY, Tien HJ, Chen SF, Horng CT, Tang HL, Jung HL, Wu MJ and Yen JH: Response of myeloid leukemia cells to luteolin is modulated by differentially expressed pituitary tumor-transforming gene 1 (pttg1) oncoprotein. Int J Mol Sci *19(4)*, 2018. PMID: 29649138. DOI: 10.3390/ijms19041173

12 Chen T, Li XF, Wang JF, Zhou S and Fang F: [Effects of luteolin on proliferation and programmed cell death of human multiple myeloma cell rpmi-8226]. Zhongguo Shi Yan Xue Ye Xue Za Zhi *26(5)*: 1425-1429, 2018. PMID: 30295262. DOI: 10.7534/j.issn.1009-2137.2018.05.028

13 Uphoff CC, Meyer C and Drexler HG: Elimination of mycoplasma from leukemia-lymphoma cell lines using antibiotics. Leukemia *16(2)*: 284-288, 2002. PMID: 11840296. DOI: 10.1038/sj.leu.2402364

14 Uphoff CC, Gignac SM and Drexler HG: Mycoplasma contamination in human leukemia cell lines. I. Comparison of various detection methods. J Immunol Methods *149(1)*: 43-53, 1992. PMID: 1374779. DOI: 10.1016/s0022-1759(12)80047-0

15 Gharbaran R, Zhang B, Valerio L, Onwumere O, Wong M, Mighty J and Redenti S: Effects of vitamin d3 and its chemical analogs on the growth of hodgkin's lymphoma, *in vitro*. BMC Res Notes *12(1)*: 216, 2019. PMID: 30961641. DOI: 10.1186/s13104-019-4241-0

16 Wrone-Smith T, Izban KF, Ergin M, Cosar EF, Hsi ED and Alkan S: Transfection of caspase-3 in the caspase-3-deficient hodgkin's disease cell line, kmh2, results in enhanced sensitivity to cd95-, trail-, and ara-c-induced apoptosis. Exp Hematol *29(5)*: 572-581, 2001. PMID: 11376869. DOI: 10.1016/s0301-472x(01)00627-0

17 Margolin N, Raybuck SA, Wilson KP, Chen W, Fox T, Gu Y and Livingston DJ: Substrate and inhibitor specificity of interleukin-1 beta-converting enzyme and related caspases. J Biol Chem *272(11)*: 7223-7228, 1997. PMID: 9054418. DOI: 10.1074/jbc.272.11.7223

18 Abu-Ghanem S, Oberkovitz G, Benharroch D, Gopas J and Livneh E: Pkceta expression contributes to the resistance of hodgkin's lymphoma cell lines to apoptosis. Cancer Biol Ther *6(9)*: 1375-1380, 2007. PMID: 17786031. DOI: 10.4161/cbt.6.9.4527

19 Alvarez-Gonzalez R, Spring H, Muller M and Burkle A: Selective loss of poly(adp-ribose) and the 85-kda fragment of poly(adp-ribose) polymerase in nucleoli during alkylation-induced apoptosis of hela cells. J Biol Chem *274(45)*: 32122-32126, 1999. PMID: 10542247. DOI: 10.1074/jbc.274.45.32122

20 Soldani C, Lazze MC, Bottone MG, Tognon G, Biggiogera M, Pellicciari CE and Scovassi AI: Poly(adp-ribose) polymerase cleavage during apoptosis: When and where? Exp Cell Res *269(2)*: 193-201, 2001. PMID: 11570811. DOI: 10.1006/excr.2001.5293

21 Segges P, Correa S, Du Rocher B, Vera-Lozada G, Krsticevic F, Arce D, Sternberg C, Abdelhay E and Hassan R: Targeting hodgkin and reed-sternberg cells with an inhibitor of heat-shock protein 90: Molecular pathways of response and potential mechanisms of resistance. Int J Mol Sci *19(3)*, 2018. PMID: 29534015. DOI: 10.3390/ijms19030836

Received July 17, 2020
Revised July 27, 2020
Accepted July 31, 2020